SAMGPT: Text-free Graph Foundation Model for Multi-domain Pre-training and Cross-domain Adaptation

Xingtong Yu
Singapore Management University
Singapore, Singapore
xingtongyu@smu.edu.sg

Zechuan Gong
University of Science and Technology of China
Hefei, China
gongzechuan@mail.ustc.edu.cn

Chang Zhou
University of Science and Technology of China
Hefei, China
gongzechuan@mail.ustc.edu.cn

Yuan Fang*
Singapore Management University
Singapore, Singapore
yfang@smu.edu.sg

Hui Zhang*
University of Science and Technology of China
Hefei, China
fzhh@ustc.edu.cn

Abstract

Graphs are able to model interconnected entities in many online services, supporting a wide range of applications on the Web. This raises an important question: How can we train a graph foundational model on multiple source domains and adapt to an unseen target domain? A major obstacle is that graphs from different domains often exhibit divergent characteristics. Some studies leverage large language models to align multiple domains based on textual descriptions associated with the graphs, limiting their applicability to text-attributed graphs. For text-free graphs, a few recent works attempt to align different feature distributions across domains, while generally neglecting structural differences. In this work, we propose a novel Structure Alignment framework for text-free Multi-domain Graph Pre-Training and cross-domain adaptation (SAMGPT). It is designed to learn multi-domain knowledge from graphs originating in multiple source domains, which can then be adapted to address applications in an unseen target domain. Specifically, we introduce a set of *structure tokens* to harmonize structure-based aggregation across source domains during the pre-training phase. Next, for cross-domain adaptation, we design dual prompts, namely, *holistic prompts* and *specific prompts*, which adapt unified multi-domain structural knowledge and fine-grained, domain-specific information, respectively, to a target domain. Finally, we conduct comprehensive experiments on seven public datasets to evaluate and analyze the effectiveness of SAMGPT.

CCS Concepts

• **Information systems → Web mining**; **Data mining**; • **Computing methodologies → Learning latent representations**.

Keywords

Graph learning, foundation models, multi-domain pre-training, prompt learning, few-shot learning.

ACM Reference Format:
Xingtong Yu, Zechuan Gong, Chang Zhou, Yuan Fang*, and Hui Zhang*. 2025. SAMGPT: Text-free Graph Foundation Model for Multi-domain Pre-training and Cross-domain Adaptation. In *Proceedings of the ACM Web Conference 2025 (WWW '25), April 28–May 2, 2025, Sydney, NSW, Australia.* ACM, New York, NY, USA, 12 pages. https://doi.org/10.1145/3696410.3714828

1 Introduction

How to build foundation models has emerged as an important question, paving a plausible path toward artificial general intelligence. In natural language processing, recent works [1, 42] have demonstrated the capabilities of universal foundation models. They are trained on a wide variety of data from multiple domains, and can be further adapted to solve a diverse range of tasks. Other than natural languages, the World Wide Web has become a vast knowledge repository, connecting an enormous amount of entities to form extensive and complex graphs. These graphs enable diverse Web applications, including social network analysis [13, 27], Web mining [2, 5], and recommendation systems [23, 28]. Given the rich graph data on the Web, can we build a universal graph model based on multi-domain graphs, to address various downstream graph-centric applications [19]?

Traditional supervised graph learning struggles to build universal models. These approaches require retraining a new graph neural network (GNN) [6, 15, 60] or graph transformer [32, 56, 66] for each new task, relying on abundant task-specific labeled data. In contrast, more recent graph pre-training methods [11, 30, 44] attempt to learn universal properties from unlabeled graphs in a self-supervised manner, which can be subsequently adapted to a downstream task with some task-specific labels through fine-tuning [14, 30, 44] or prompt learning [21, 40, 62]. However, in most existing graph pre-training approaches, the pre-training and downstream graphs originate from the same dataset [21, 40, 44, 57], a practice we refer to as *single-domain* methods, which fall short of building a universal, *multi-domain* graph model from multiple graph datasets.

[*] Corresponding authors.

WWW '25, Sydney, NSW, Australia.

ACM ISBN 979-8-4007-1274-6/25/04
https://doi.org/10.1145/3696410.3714828

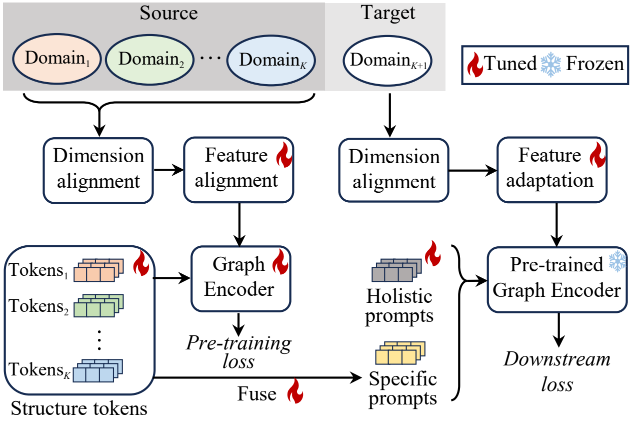

(a) Multi-domain pre-training (b) Cross-domain adaptation

Figure 1: Motivation of SAMGPT.

Research problem. Thus, it is crucial to pre-train a graph model on a wide range of multi-domain (*i.e.*, multi-dataset) graphs and achieve cross-domain adaptation. However, graph structures from different datasets often exhibit markedly distinct characteristics. For instance, the structural patterns in a social network might not be directly applicable to a citation or e-commerce graph. Such diversity poses significant challenges in integrating graphs from multiple domains and adapting prior knowledge to different domains. Although some studies have explored cross-domain adaptation from a single source domain [4, 9, 45, 47, 55], they do not exploit multiple source domains. Another line of work [18, 41, 53] employs large language models to extract and utilize multi-domain knowledge based on textual descriptions associated with graphs, using text as a universal medium to bridge different domains. However, this limits their applicability to text-attributed graphs [49, 70] and cannot be extended to general graphs without textual descriptions. Few recent studies [65, 69] have explored multi-domain pre-training on text-free graphs, but they focus on aligning the divergent feature spaces and homophily patterns across multi-domain graphs, while overlooking the structural differences across domains.

Challenges and insights. In this paper, we propose SAMGPT, a graph foundation model with **S**tructural **A**lignment for text-free **M**ulti-domain **G**raph **P**re-**T**raining, to facilitate cross-domain adaptation. This is non-trivial due to two key challenges.

First, *how do we harmonize structural variance across multiple domains during pre-training?* Graphs from different domains often exhibit distinct structural and topological characteristics, such as average node degree, shortest path length and clustering coefficient, as depicted in Table 1. Thus, merging multi-domain graphs without structure alignment during pre-training may cause interference rather than synergy, leading to suboptimal performance. In SAMGPT, we propose *structure tokens* to align structural distributions across multiple domains, as shown in Fig. 1(a). Each domain is equipped with a series of structure tokens, which modify the structure-based aggregation in each layer of the graph encoder. These tokens are learnable vectors that capture domain-specific structural patterns, enabling the model to accommodate the unique structural characteristics of each domain during pre-training.

Second, *how do we adapt multi-domain prior structural knowledge to cross-domain downstream tasks?* Multi-domain prior knowledge includes not only holistic knowledge across source domains, but also domain-specific knowledge from each domain. Therefore, in SAMGPT, we propose dual *structural prompts*, comprising a set of *holistic prompts* and a set of *specific prompts*, thus facilitating the adaptation of both holistic and domain-specific knowledge to downstream tasks, as illustrated in Fig. 1(b). On one hand, the holistic prompts consist of learnable vectors that holistically align the target domain's structural characteristics with the unified pre-trained knowledge from all source domains. On the other hand, specific prompts integrate multi-domain structure tokens in a learnable mixture to align the target domain with knowledge from each source domain, capturing domain-specific structural information for finer-grained adaptation.

Contributions. In summary, we make the following contributions in this work. (1) We propose SAMGPT, a text-free graph foundation model with structure alignment for multi-domain graph pre-training and cross-domain adaptation. (2) For pre-training, we propose structure tokens to align structural distributions across domains, training a universal foundation model with multi-domain graphs. (3) For downstream adaptation, we propose a dual-prompt strategy, using holistic prompts to leverage holistic prior structural knowledge and specific prompts to facilitate finer-grained, domain-specific structural adaptation. (4) We conduct extensive experiments on seven benchmark datasets, demonstrating the superior performance of SAMGPT compared to state-of-the-art methods.

2 Related Work

We review related literature on pre-training, cross-domain transfer learning, and multi-domain pre-training for graph data.

Graph pre-training. Graph pre-training methods aim to extract inherent properties of graphs, often utilizing self-supervised learning approaches, which can be either generative [10–12, 16] or contrastive [17, 44, 52, 54]. The pre-trained model is then employed to address downstream tasks through fine-tuning [30, 44, 57] or parameter-efficient adaptation methods, notably prompt-based learning [7, 21, 39, 59]. However, these methods typically assume that the pre-training and downstream graphs originate from the same domain, such as different subgraphs of a large graph [57, 61] or collections of similar graphs within the same dataset [11, 30], failing to account for multiple domains in either pre-training or downstream graphs.

Graph cross-domain transfer. This line of work aims to transfer single-source domain knowledge to a different target domain by leveraging domain-invariant properties across domains [4, 9, 45, 47]. However, they rely exclusively on a single source domain, failing to harness the extensive knowledge available across multiple domains. Additionally, these approaches are often tailored to specific tasks or domains [4, 9, 45, 47], limiting their generalization.

Multi-domain graph pre-training. In the context of graphs from multiple domains, recent works [18, 41, 53] utilize large language models to align node features from different domains through textual descriptions, thereby limiting their applicability to text-attributed graphs [50, 67, 70]. For graphs without textual attributes, GraphControl [72] applies ControlNet [68] to incorporate target domain node features with the pre-trained model, while neglecting the alignment among multiple source domains. Another recent study proposes GCOPE [69], which employs domain-specific virtual nodes that interconnect nodes across domains, facilitating the alignment of feature distribution and homophily patterns. Meanwhile, MDGPT [65] pre-trains domain-specific tokens to align feature semantics across various domains. However, these studies do not account for structural variance across different domains, hindering their effectiveness in integrating multi-domain knowledge. On a related front, multi-task pre-training techniques [48, 64] employ pretext tokens for each pre-training task. It is important to note that they address a distinct problem, aiming to overcome potential interference among multiple tasks within a single domain, rather than interference across multiple domains.

3 Preliminaries

In this section, we provide technical background, and outline the scope of our work.

Graph encoder. A *graph* is defined as $G = (V, E, \mathbf{X})$, where V is the set of nodes, E is the set of edges, and $\mathbf{X} \in \mathbb{R}^{|V|\times d}$ is the node feature matrix with each row $\mathbf{x}_i$ representing the feature vector of node $v_i \in V$. A collection of graphs is denoted as $\mathcal{G}$.

Message-passing GNNs are a common choice for encoding graph representations [51]. Specifically, each node updates its embedding by receiving and aggregating features or embeddings from its neighbors. By stacking such message-passing layers, information can propagate recursively throughout the graph. Therefore, the node embeddings are encoded based on both input features and graph structure. Let us denote the embedding of node v at the l-th layer as $\mathbf{h}_v^l$, which is derived from the features or embeddings in the preceding layer as follows.

$$\mathbf{h}_v^l = \mathtt{Aggr}(\mathbf{h}_v^{l-1}, \{\mathbf{h}_u^{l-1} : u \in \mathcal{N}_v\}; \theta^l), \tag{1}$$

where $\mathcal{N}_v$ denotes the set of neighboring nodes of v, θ^l represents the learnable parameters in layer l, and $\mathtt{Aggr}(\cdot)$ stands for the neighborhood aggregation function. In the first layer, the node embedding $\mathbf{h}_v^0$ is initialized as the input feature vector $\mathbf{x}_v$. We denote the output node embedding after the last layer as $\mathbf{h}_v$, which is a row in the node embedding matrix $\mathbf{H}$. Overall, the multi-layer message-passing process can be abstracted as a *graph encoder*, as follows.

$$\mathbf{H} = \mathtt{GE}(G, \mathbf{X}; \Theta), \tag{2}$$

where $\mathtt{GE}$ denotes a graph encoder, $\Theta = \{\theta^1, \theta^2, \ldots\}$ is the full set of trainable parameters for the graph encoder.

Multi-domain pre-training with feature alignment. Consider a set of unlabeled graphs $\mathcal{G}_S = \{G_1, G_2, \ldots, G_K\}$ for pre-training, where each graph G_i belongs to a specific *source domain* $D_{S_i} \in \mathcal{D}_S$. Thus, we have graph-domain pairs $\{(G_i, D_{S_i}) : i \in \{1, 2, \ldots, K\}\}$.

As different domains exhibit distinct feature distributions, previous works [58, 69] have proposed solutions to align feature dimensions and semantics, which can be directly employed in our work. Given a graph $G_i = (V_i, E_i, \mathbf{X}_i)$ from the source domain D_{S_i}, we first align the dimensions of its feature matrix:

$$\tilde{\mathbf{X}}_i = \mathtt{DAL}_{S_i}(\mathbf{X}_i), \tag{3}$$

where $\mathtt{DAL}_{S_i} : \mathbb{R}^{|V|\times d_{S_i}} \to \mathbb{R}^{|V|\times \tilde{d}}$ is the dimension alignment function for domain D_{S_i}, transforming the original dimension d_{S_i} to a common dimension $\tilde{d}$ across domains. We implement $\mathtt{DAL}$ as singular value decomposition [37] following prior art [58, 69]. Next, given the source-domain graphs $\mathcal{G}_S$ with their dimension-aligned features $\tilde{\mathcal{X}}_S = \{\tilde{\mathbf{X}}_i : G_i \in \mathcal{G}_S\}$, we further align the features to unify their semantic space across various domains. Letting $\mathtt{FAL}$ denote the feature alignment procedure, we pre-train a graph encoder with feature alignment:

$$\mathbf{H}^{\mathtt{FAL}} = \mathtt{GE}(\mathtt{FAL}(\mathcal{G}_S, \tilde{\mathcal{X}}_S; \Psi); \Theta), \tag{4}$$

where Ψ denotes the learnable parameters in $\mathtt{FAL}$, and $\mathbf{H}^{\mathtt{FAL}}$ is the output node embedding matrix with feature alignment. While any feature alignment model can be employed [58, 69], we follow the work of Yu et al. [58] due to its superior performance.

Cross-domain task with feature adaptation. For each downstream task, consider a set of graphs $\mathcal{G}_T$ belonging to a target domain D_T. The task is *cross-domain* if the target domain is *unseen* during pre-training, *i.e.*, $\forall i\ D_T \neq D_{S_i}$. Again, since the target domain may exhibit different feature characteristics from the source domains, previous works [65, 69] have proposed feature adaptation strategies to transfer prior multi-domain knowledge to the target domain, which can be directly integrated into our work. Specifically, we first employ the same dimension alignment method used in the pre-training phase, transforming the feature matrix of a downstream graph $G = (V, E, \mathbf{X}) \in \mathcal{G}_T$ to $\tilde{\mathbf{X}} = \mathtt{DAL}_T(\mathbf{X})$. We then employ a feature adaptation technique $\mathtt{FAD}$ to adapt the pre-trained model to the target domain, as follow.

$$\mathbf{H}^{\mathtt{FAD}} = \mathtt{GE}(\mathtt{FAD}(G, \tilde{\mathbf{X}}; \Gamma); \Theta_{\text{pre}}), \tag{5}$$

where Γ denotes the learnable parameters in $\mathtt{FAD}$, and Θ_{pre} is the pre-trained weights in graph encoder $\mathtt{GE}$. Here we implement $\mathtt{FAD}$ following Yu et al. [58], which is paired with the feature alignment method in pre-training.

Our scope: Few-shot classification. For the downstream applications, we aim to solve *few-shot* node and graph classification tasks. For node classification, given a graph $G = (V, E, \mathbf{X}) \in \mathcal{G}_T$, each node $v \in V$ is associated with a label $y \in Y$, where Y denotes the set of node classes. For graph classification over a set of graphs $\mathcal{G}_T$, each graph $G \in \mathcal{G}_T$ is associated with a label $y \in Y$, where Y denotes the set of graph classes. An m-shot classification task consists of only m labeled examples per class, along with an arbitrary number of unlabeled examples for testing.

In particular, we focus on *low-shot* settings, where m is a small number (*e.g.*, $m \leq 5$), reflecting real-world scenarios where labeled data are expensive or difficult to obtain. Due to the parameter-efficient nature of prompt learning, many previous methods for prompt learning on graphs [21, 40, 59, 65, 69] also emphasize this setting. It is expected that, as more task-specific labeled data become available, conventional fine-tuning or supervised approaches may become sufficient.

4 Proposed Approach: SAMGPT

In this section, we present SAMGPT, beginning with an overview and then delving into the details of multi-domain pre-training and cross-domain adaptation.

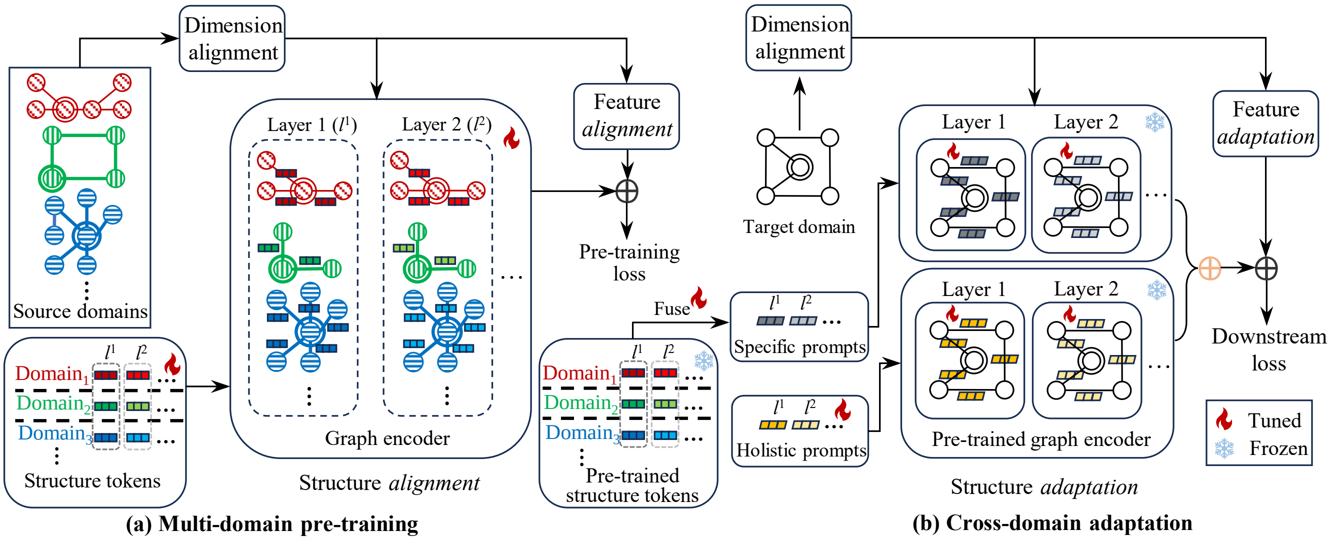

Figure 2: Overall framework of SAMGPT.

4.1 Overall Framework

SAMGPT consists of two phases: multi-domain pre-training, and cross-domain adaptation, as shown in Fig. 2.

In the pre-training phase, as depicted in Fig. 2(a), we first align the feature distributions from multiple source domains following previous work [65, 69]. Next, we introduce a set of *structure tokens* designed to align the structural distributions across diverse domains. These tokens are domain-specific and are integrated into each layer of the graph encoder, modifying the structure-based aggregation at each layer. Finally, the structure token-enhanced graph encoder is pre-trained using a self-supervised loss [21].

In the adaptation phase, as shown in Fig. 2(b), we first align the feature dimension of the target domain with that of the source domains. Then, we introduce *dual prompts*. The first type, *holistic prompts*, are learnable vectors that integrate the target domain with the holistic structural knowledge from all source domains. The second type, *specific prompts*, comprise learnable mixtures of pre-trained structure tokens that incorporate domain-specific topological information tailored to the target domain. These prompts are applied to each layer of the graph encoder to adjust the structure-based aggregation, while keeping the pre-trained weights of the graph encoder frozen.

4.2 Multi-domain Graph Pre-training with Structure Alignment

As defined in Sect. 3, we are given a set of pre-training graphs from multiple source domains, $\mathcal{G}_S$. As both the features and structures of these domains can exhibit divergent distributions, effective integration of these multi-domain graphs requires aligning both. As our work focuses on structure alignment, we follow previous feature alignment methods [58, 69], as outlined in the preliminaries.

Structure alignment. Recall that in the graph encoder, node representations are updated layer-wise through a structure-based aggregation. Each layer captures different levels of structural information. For example, the first layer aggregates one-hop neighborhood information, while the second layer incorporates a broader two-hop neighborhoods. These layer-wise structural patterns may vary significantly across domains.

Therefore, to unify the structural characteristics in multiple source domains, we introduce learnable *structure tokens*. For each domain D_{S_i}, we inject a series of structure tokens $\mathcal{T}_{S_i} = \{\mathbf{t}^l_{S_i} : l \in \{1, \dots, L\}\}$ into the graph encoder, where L denotes the number of layers. Specifically, when encoding the graph $G_i = (V_i, E_i, \tilde{\mathbf{X}}_i)$ in D_{S_i}, we assign structure token $\mathbf{t}^l_{S_i}$ to the l-th layer, guiding structure-based aggregation:

$$\mathbf{h}^l_v = \mathtt{Aggr}(\mathbf{h}^{l-1}_v, \{\mathbf{t}^l_{S_i} \odot \mathbf{h}^{l-1}_u : u \in \mathcal{N}_v\}; \theta^l), \ \forall v \in V_i, \tag{6}$$

where $\odot$ represents element-wise multiplication. Note that the graph encoders for feature alignment and structure alignment on all graphs share the same parameters Θ. Let $\mathbf{H}^{\mathsf{SAL}}_i$ denote the structure-aligned output node embedding matrix for G_i in D_{S_i}, following the aggregation in Eq. (6). In general, each source domain is attached with its own set of structure tokens, which are applied to modify the aggregation on the graph in the corresponding domain. By stacking the structure-aligned output matrix across graphs in all domains, we obtain the overall structure-aligned embedding matrix, $\mathbf{H}^{\mathsf{SAL}} = \mathtt{Stack}(\mathbf{H}^{\mathsf{SAL}}_1, \dots, \mathbf{H}^{\mathsf{SAL}}_K)$.

Finally, we fuse $\mathbf{H}^{\mathsf{SAL}}$ with $\mathbf{H}^{\mathsf{FAL}}$ in Eq. (4) to obtain the multi-domain node embedding matrix $\mathbf{H}$, incorporating both feature and structure alignment, as shown below.

$$\mathbf{H}^{\mathsf{AL}} = \mathbf{H}^{\mathsf{FAL}} + \alpha \mathbf{H}^{\mathsf{SAL}}, \tag{7}$$

where $\alpha > 0$ is a hyperparameter.

Pre-training loss. We leverage a universal task template based on subgraph similarity calculation [21, 59], which ensures compatibility across different tasks such as node classification and graph classification. As demonstrated in GraphPrompt+ [59], prevailing contrastive pre-training objectives can be unified under this template, making them suitable choices for the pre-training loss in

SAMGPT. In general, we can adopt the following form of contrastive loss in pre-training.

$$\mathcal{L}_{\text{pre}}(O;\Theta,\mathcal{T},\Psi) = -\sum\nolimits_{o\in O} \ln \frac{\sum_{a\in \text{Pos}_o}\exp(\texttt{sim}(\mathbf{h}_a,\mathbf{h}_o)/\tau)}{\sum_{b\in\text{Neg}_o}\exp(\texttt{sim}(\mathbf{h}_b,\mathbf{h}_o)/\tau)}, \tag{8}$$

where O denotes the set of observed graph element in pre-training, $a \in \text{pos}_o, b \in \text{neg}_o$ represent the positive or negative instance of o, respectively, and $\mathbf{h}_o, \mathbf{h}_a, \mathbf{h}_b$ are their corresponding embeddings. Furthermore, $\texttt{sim}(\cdot,\cdot)$ is a similarity function, such as cosine similarity [31] in our implementation, and $\tau > 0$ is a temperature hyperparameter. Note that SAMGPT is flexible in the materialization of o, a, b to realize different contrastive losses [59]. Our experiments adopt GraphCL [57], where o is the original graph G, and a, b represent two different augmentations of G. Hence, $\mathbf{h}_o, \mathbf{h}_a, \mathbf{h}_b$ are the corresponding graph embeddings, which can be obtained through a readout operation [21] on the aligned node embeddings in $\mathbf{H}^{\mathsf{AL}}$.

The pre-training loss is optimized by updating the weights of graph encoder Θ, structure tokens across all source domains $\mathcal{T} = \{\mathcal{T}_{S_1}, \dots, \mathcal{T}_{S_K}\}$, and feature alignment parameters Ψ.

4.3 Cross-domain Structure Adaptation

Beyond multi-domain pre-training, another challenge lies in cross-domain adaptation. Given a model pre-trained on graphs $\mathcal{G}_S$ from source domains $\mathcal{D}_S$, we aim to adapt it to a downstream task on graphs $\mathcal{G}_T$ from a target domain $D_T \notin \mathcal{D}_S$. As this work focuses on structure adaptation, we directly apply previous work [58] for feature adaptation, as outlined in Sect. 3.

For structure adaptation, we propose *dual prompts*, consisting of *holistic prompts* and *specific prompts*. On one hand, the holistic prompts are designed to holistically utilize the pre-trained structural knowledge from all source domains. On the other hand, the specific prompts combine multi-domain structure tokens through a learnable mixture, adapting fine-grained, domain-specific structural knowledge to the target domain.

Holistic prompts. To transfer the holistic multi-domain structural knowledge to a downstream task, we propose a set of holistic prompts designed to align the target domain D_T with the model pre-trained on the source domains $\mathcal{D}_S$. Like any pre-training framework, we encode a downstream graph $G = (V, E, \tilde{\mathbf{X}})$ using the pre-trained graph encoder with frozen layer-wise weights $\Theta_{\text{pre}} = \{\theta^1_{\text{pre}}, \dots, \theta^L_{\text{pre}}\}$. However, the key difference is that we inject a series of learnable vectors $\mathcal{P}_{\text{hol}} = \{\mathbf{p}^1_{\text{hol}}, \dots, \mathbf{p}^L_{\text{hol}}\}$ as holistic prompts into the downstream structure-based aggregation:

$$\mathbf{h}^l_v = \texttt{Aggr}(\mathbf{h}^{l-1}_v, \{\mathbf{p}^l_{\text{hol}} \odot \mathbf{h}^{l-1}_u : u \in \mathcal{N}_v\}; \theta^l_{\text{pre}}),\ \forall v \in V. \tag{9}$$

The final layer outputs a holistic node embedding matrix for the downstream graph G, denoted as $\mathbf{H}^{\text{hol}}$.

Specific prompts. In contrast to the holistic prompts, specific prompts are designed to adapt structural knowledge specific to each source domain. Since knowledge from related source domains is likely to be more applicable, it is essential to align the target domain with different source domains to varying extents, prioritizing the most relevant ones. Consequently, we define specific prompts as $\mathcal{P}_{\text{spe}} = \{\mathbf{p}^1_{\text{spe}}, \dots, \mathbf{p}^L_{\text{spe}}\}$, which will also be injected into different layers of the pre-trained graph encoder. Specifically, in the l-th layer, $\mathbf{p}^l_{\text{spe}}$ is a combination of $\{\mathbf{t}^l_{S_1}, \dots, \mathbf{t}^l_{S_K}\}$, the pre-trained structure tokens in the corresponding layer across all source domains $D_{S_i} \in \mathcal{D}_S$. Formally, we define

$$\mathbf{p}^l_{\text{spe}} = \sum\nolimits_{i=1}^K \lambda^l_i \mathbf{t}^l_{S_i}, \tag{10}$$

where $\Lambda^l = \{\lambda^l_1, \dots, \lambda^l_K\}$ are learnable coefficients. Thus, the full set of learnable parameters for the specific prompts is $\Lambda = \{\Lambda^1, \dots, \Lambda^L\}$. Subsequently, specific prompts modify the structure-based aggregation in the same way as in Eq. (9), while freezing the pre-trained weights of the graph encoder. Similarly, we denote the output node embedding matrix based on the specific prompts as $\mathbf{H}^{\text{spe}}$.

Prompt tuning. To leverage both holistic multi-domain and domain-specific structural knowledge from the pre-trained model, we fuse the output embedding matrices obtained via holistic prompts and specific prompts as follows.

$$\mathbf{H}^{\mathsf{SAD}} = \mathbf{H}^{\text{hol}} + \beta\mathbf{H}^{\text{spe}}, \tag{11}$$

where $\beta > 0$ is a hyperparameter. Further incorporating feature adaptation in Eq. (5), we obtain the overall node embedding matrix with both feature and structure adaptations, given by

$$\mathbf{H}^{\mathsf{AD}} = \mathbf{H}^{\mathsf{FAD}} + \alpha\mathbf{H}^{\mathsf{SAD}}. \tag{12}$$

Here, α is the same hyperparameter used in Eq. (7), as both share the objective of integrating the feature and structure counterparts.

For downstream node and graph classification tasks, the loss function $\mathcal{L}_{\text{down}}$ is formulated based on the same task template with subgraph similarity [21], akin to the pre-training loss $\mathcal{L}_{\text{pre}}$. Let $\Omega = \{(x_1, y_1), (x_2, y_2), \dots\}$ represent the labeled training set, where each x_i is either a node or graph instance, and $y_i \in Y$ is its respective class from the set Y. Subsequently, we optimize the following cross-domain adaptation loss:

$$\mathcal{L}_{\text{down}}(\Omega;\mathcal{P}_{\text{hol}},\Lambda,\Gamma) = -\sum\nolimits_{(x_i,y_i)\in\Omega}\ln\frac{\exp(\text{sim}(\mathbf{h}_{x_i},\mathbf{h}_{y_i})/\tau)}{\sum_{y\in Y}\exp(\text{sim}(\mathbf{h}_{x_i},\mathbf{h}_y)/\tau)}. \tag{13}$$

Here, $\mathbf{h}_{x_i}$ represents the adapted embedding of the node or graph x_i based on $\mathbf{H}^{\mathsf{AD}}$, where a readout operation on $\mathbf{H}^{\mathsf{AD}}$ is required if x_i is a graph. Additionally, $\mathbf{h}_y$ denotes the prototype embedding for class y, which is calculated as the average embeddings of all training instances of class y.

We outline the key steps for prompt tuning in Algorithm 1, Appendix A and assess its complexity in Appendix B.

5 Experiments

In this section, we conduct experiments to assess the performance of SAMGPT and analyze its empirical results.

5.1 Experimental Setup

Datasets. We conduct experiments on seven benchmark datasets. (1) *Cora* [26], (2) *Citeseer* [35] and (3) *Pubmed* [35] are scientific paper citation networks from different fields, including computer science and biomedical research. Nodes represent academic publications and edges denote citation relationships. (4) *Photo* [36] and (5) *Computers* [25] are both e-commerce networks from Amazon in different categories, namely, photography and computer related products. Nodes represent products and edges signify frequent co-purchases between products. (6) *Facebook* [33] is a Web graph, where nodes represent official Facebook pages while the links are

Table 1: Summary of datasets.

	Nodes	Edges	Feature dimension	Node classes	Avg. nd	Avg. spl	Avg. cc
Cora	2,708	10,556	1,433	7	3.89	6.30	0.24
Citeseer	3,327	9,104	3,703	6	2.73	9.31	0.14
Pubmed	19,717	88,648	500	3	4.49	6.33	0.06
Photo	7,650	238,162	745	8	31.13	4.05	0.40
Computers	13,752	491,722	767	10	35.75	3.38	0.34
Facebook	22,470	342,004	128	4	15.22	4.97	0.35
LastFM	7,624	55,612	128	18	7.29	5.23	0.21

nd: node degree, spl: shortest path length [3], cc: clustering coefficient [8].

mutual likes between these pages. (7) *LastFM* [34] is a social network, where nodes denote users and edges represent interactions such as follower relationships. Note that each domain comprises a single graph. We summary these datasets in Table 1 and present additional details in Appendix C.

Setup of pre-training and downstream tasks. Following previous work [65, 69], we treat each dataset as a distinct domain. Among the seven datasets (or domains), we use each of them as the target domain while leveraging the remaining six as source domains for pre-training.

On each target domain, we conduct m-shot *node classification* and *graph classification*, where m labeled nodes or graphs per class are randomly selected for downstream prompt tuning. Given that each dataset comprises a single graph, performing graph classification on whole graphs is not feasible. Therefore, following previous works [22, 61, 63], we generate a series of graphs by constructing ego-networks centered on the labeled nodes within each dataset, and set up graph classification on these ego-networks, with each network labeled according to its central node. Note that the graph encoder is pre-trained only once for each set of source domains, and subsequently utilized across all downstream tasks. We generate 100 m-shot tasks for both node classification and graph classification by repeatedly sampling m labeled nodes or graphs per class for 100 times. Each task is executed with five different random seeds, leading to a total of 500 outcomes for each classification type. We use accuracy as the evaluation metric, as each task is class-balanced [20, 21, 46, 59], and report the average accuracy and standard deviation over these 500 outcomes.

Baselines. We compare the performance of SAMGPT against state-of-the-art methods in four broad groups, as follows.

(1) *End-to-end graph neural networks*: GCN [15] and GAT [43] aggregate information from neighboring nodes to update node representations. For each task, they are trained from scratch in a supervised fashion without pre-training.

(2) *Graph pre-training models*: DGI [44], InfoGraph [38][1] and GraphCL [57] first pre-train a graph encoder to capture the inherent properties of the graphs, and then fine-tune a classifier on the downstream task while freezing the pre-trained model. GPPT[2] [39], GPF [7] and GraphPrompt [21] employ a universal task template to unify self-supervised pre-training and downstream tasks, and tune a single prompt on downstream tasks.

(3) *Graph cross-domain models*: Hassani [9] pre-trains a GNN on a single source domain by incorporating both contextual and topological views, which facilitates cross-domain adaptation for downstream tasks.

(4) *Multi-domain pre-training models*: GCOPE [69] performs multi-domain pre-training, and subsequently adapts to cross-domain tasks through either fine-tuning a classification head or prompt tuning. We opt for fine-tuning as it yields superior performance.

Note that the above graph pre-training and cross-domain approaches are originally designed for pre-training on a single source domain. For a fair comparison, we directly merge the multi-domain graphs and apply dimension alignment for them, as in SAMGPT. Further descriptions of the baselines are provided in Appendix D, with implementation details in Appendix E.

5.2 Performance Evaluation

We first compare SAMGPT and the baseline methods on one-shot node and graph classification tasks, and then investigate the effect of increasing the number of shots.

One-shot performance. Tables 2 and 3 show the results of one-shot node and graph classification tasks. We observe that, first, SAMGPT achieves outstanding performance in both node and graph classification across various target domains, demonstrating the effectiveness of our proposed structure tokens in multi-domain pre-training and dual prompts in cross-domain adaptation. We defer analysis of the quantitative contributions of these components to the ablation studies in Sect. 5.3. Second, another text-free multi-domain pre-training method, GCOPE, significantly lags behind SAMGPT because it only performs alignment and adaptation on feature and homophily patterns, without accounting for structural differences across domains. This further emphasizes the importance of our structure tokens and dual prompts. Third, graph pre-training methods generally outperform the end-to-end GCN and GAT, showcasing the benefits of pre-training on unlabeled graphs.

Few-shot performance. To evaluate the performance of SAMGPT with more labeled data, we vary the number of shots, m, in both node and graph classification tasks. We compare SAMGPT to two competitive baselines, GraphPrompt and GCOPE, with results reported in Fig. 3, where error bars represent the standard deviation. We observe that SAMGPT consistently outperforms the baselines in low-shot settings (*e.g.*, $m \leq 5$). When further increasing the number of shots, SAMGPT still performs best in general, although it may be on par with GCOPE in some cases when m approaches 10. This is not surprising, since the advantage of SAMGPT may diminish as more supervision becomes available.

5.3 Ablation Studies

To understand the impact of each component in SAMGPT, we perform two ablation studies.

Data ablation. We evaluate the impact of incorporating more source domains by incrementally adding *Citeseer*, *LastFM*, *Photo*, and *Facebook*, in this order, to the pre-training, while fixing *Cora* as

[1] Original DGI only operates at the node level, while InfoGraph extends it to the graph level. We apply DGI to node classification, and InfoGraph to graph classification.

[2] GPPT is tailored for node classification task and is not applicable to graph classification. Thus, in our experiments, we only use GPPT for node classification.

Table 2: Accuracy (%) of one-shot *node classification* with standard deviations. Each column represents a target domain, using other columns as source domains. The best method in each column is bolded, and the runner-up is underlined.

Method \ Target domain	Cora	Citeseer	Pubmed	Photo	Computers	Facebook	LastFM
GCN	29.53 ± 7.56	26.29 ± 6.50	23.32 ± 11.56	26.96 ± 12.94	24.40 ± 5.62	20.45 ± 5.62	9.21 ± 3.11
GAT	24.27 ± 9.26	21.56 ± 8.09	22.28 ± 9.76	17.85 ± 10.22	23.03 ± 12.12	29.27 ± 6.47	9.01 ± 2.61
DGI	33.40 ± 10.48	25.80 ± 8.27	47.22 ± 9.50	30.89 ± 10.54	25.75 ± 12.45	34.36 ± 9.57	14.14 ± 6.31
GraphCL	27.72 ± 9.37	35.02 ± 8.46	48.89 ± 9.03	34.78 ± 11.56	23.79 ± 12.28	34.85 ± 7.07	18.93 ± 7.32
GPPT	27.18 ± 4.88	25.90 ± 4.68	39.82 ± 8.79	31.58 ± 10.27	19.94 ± 9.61	34.73 ± 3.99	20.98 ± 3.98
GraphPrompt	28.26 ± 12.68	32.51 ± 8.73	47.47 ± 9.15	48.11 ± 9.89	42.82 ± 11.67	40.44 ± 9.68	19.84 ± 7.23
GPF	32.17 ± 6.56	36.79 ± 7.70	41.28 ± 8.14	47.47 ± 8.19	35.75 ± 7.12	40.45 ± 6.34	27.26 ± 5.50
Hassani	33.35 ± 6.93	33.66 ± 7.24	39.87 ± 8.16	48.48 ± 7.07	39.99 ± 7.91	37.70 ± 5.79	27.16 ± 4.94
GCOPE	35.62 ± 11.93	**38.33** ± 9.28	45.38 ± 9.87	52.87 ± 9.19	45.65 ± 10.69	40.63 ± 8.50	28.84 ± 7.59
SAMGPT	**47.80** ± 11.88	36.38 ± 9.10	**50.25** ± 10.43	**58.71** ± 8.69	**48.22** ± 8.17	**42.70** ± 8.73	**33.36** ± 8.11

Table 3: Accuracy (%) of one-shot *graph classification* with standard deviations. Each column represents a target domain, using other columns as source domains. The best method in each column is bolded, and the runner-up is underlined.

Method \ Target domain	Cora	Citeseer	Pubmed	Photo	Computers	Facebook	LastFM
GCN	30.64 ± 10.31	26.90 ± 7.15	38.84 ± 11.82	15.60 ± 8.77	21.94 ± 14.51	31.33 ± 9.47	28.83 ± 9.60
GAT	27.80 ± 7.85	27.50 ± 7.13	21.66 ± 8.70	15.74 ± 7.62	16.02 ± 13.46	21.20 ± 7.31	27.80 ± 7.85
InfoGraph	34.98 ± 10.15	35.87 ± 9.84	48.67 ± 12.29	25.70 ± 11.73	19.02 ± 14.09	31.26 ± 9.65	23.29 ± 7.99
GraphCL	42.70 ± 10.64	36.66 ± 8.67	47.53 ± 11.52	33.07 ± 12.31	16.02 ± 13.47	21.99 ± 13.00	21.30 ± 10.45
GraphPrompt	37.38 ± 14.03	36.66 ± 9.19	**49.55** ± 10.25	50.79 ± 12.31	43.09 ± 11.45	41.71 ± 10.61	32.62 ± 8.54
GPF	39.62 ± 8.52	36.73 ± 7.66	45.08 ± 10.36	47.57 ± 10.16	35.70 ± 8.71	34.84 ± 5.14	34.31 ± 7.05
Hassani	36.86 ± 10.74	35.78 ± 8.80	43.97 ± 13.27	41.55 ± 13.08	29.49 ± 13.86	35.57 ± 9.00	25.39 ± 8.14
GCOPE	38.85 ± 10.99	**39.93** ± 9.82	47.05 ± 11.74	53.93 ± 9.74	45.60 ± 10.96	40.26 ± 9.53	34.68 ± 7.70
SAMGPT	**55.35** ± 13.62	38.75 ± 9.40	48.69 ± 10.16	**58.75** ± 11.67	**48.72** ± 11.18	**43.71** ± 9.54	**48.28** ± 9.72

Table 4: Data ablation study with an increasing number of source domains, while fixing *Cora* as the target domain.

Method	Number of source domains			
	1	2	3	4
GraphPrompt	35.53±12.06	37.13±11.79	36.90±11.23	38.54±11.84
GCOPE	39.47±12.14	36.63± 9.46	35.28±11.99	38.61±12.74
SAMGPT	**40.43**±11.00	**41.97**±11.01	**42.30**±11.56	**45.95**±12.96

the target domain. We present one-shot node classification performance of SAMGPT and two competitive baselines, namely, GraphPrompt and GCOPE, in Table 4. Across the columns, 1 represents using *Citeseer* as the single source domain, while 2 represents using *Citeseer* and *LastFM* as the source domains, *etc.*

We make the following observations. First, SAMGPT is superior across different numbers of source domains, demonstrating its robustness to varying configurations of the source domains. Second, both GraphPrompt and GCOPE often perform worse as more datasets are added due to the negligence of structural discrepancies in various domains. In contrast, SAMGPT exhibits consistent improvement with the addition of more source domains, validating the effectiveness of our structure alignment and adaptation.

Model ablation. We analyze variants of SAMGPT by removing structure tokens, holistic prompts and specific prompts. We report the results of these variants and SAMGPT in Table 5. Note that Variant 1, which lacks our structural alignment design, is equivalent to the feature alignment method MDGPT [65].

The results confirm that each component plays an important role. First, the use of structure tokens is essential. Notably, Variant 3 consistently outperforms Variant 1 and 2, both of which do not employ structure tokens, demonstrating the effectiveness of structure tokens in aligning multi-domain structural knowledge. Second, removing specific prompts leads to a drop in performance, evident from the superior accuracy of Variants 2 over Variant 1, and SAMGPT over Variant 4. This indicates the significance of leveraging source domain-specific structural knowledge for effective cross-domain adaptation. Third, holistic prompts prove to be useful, as Variant 4 often outperforms Variant 3, highlighting the significance of incorporating holistic multi-domain structural information via holistic prompts. These key components together enable SAMGPT to achieve optimal performance.

5.4 Homophily Sensitivity

Apart from feature and structural differences, graphs also exhibit varying homophily and heterophily patterns based on whether linked nodes share the same attribute [24, 63, 71]. To further assess

Table 5: Model ablation study on key components of SAMGPT.

Methods	Structure tokens	Holistic prompts	Specific prompts	Target domain for node classification			Target domain for graph classification		
				Cora	Photo	Facebook	Cora	Photo	Facebook
VARIANT 1	×	×	×	36.36 ± 12.71	49.10 ± 9.94	35.36 ± 9.06	45.44 ± 13.47	52.45 ± 12.37	38.74 ± 10.26
VARIANT 2	×	×	✓	40.62 ± 11.79	56.23 ± 9.04	39.80 ± 10.39	45.63 ± 13.52	57.78 ± 11.64	42.22 ± 10.95
VARIANT 3	✓	×	×	44.26 ± 10.92	56.61 ± 10.14	41.11 ± 8.34	52.88 ± 12.25	58.14 ± 12.01	43.12 ± 9.76
VARIANT 4	✓	✓	×	46.10 ± 12.02	57.76 ± 10.00	40.46 ± 8.89	54.52 ± 14.32	58.12 ± 12.30	43.15 ± 10.12
SAMGPT	✓	✓	✓	**47.80** ± 11.88	**58.71** ± 8.69	**42.70** ± 8.73	**55.35** ± 13.62	**58.75** ± 11.67	**43.71** ± 9.54

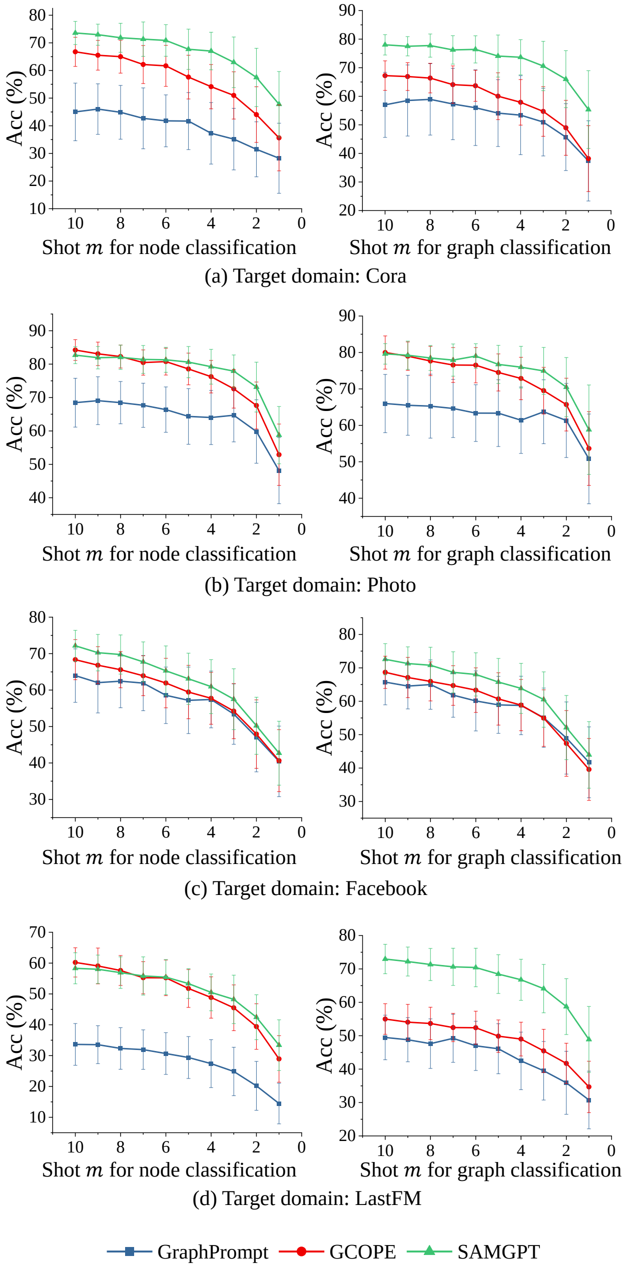

(a) Target domain: Cora

(b) Target domain: Photo

(c) Target domain: Facebook

(d) Target domain: LastFM

Figure 3: Impact of number of shots on node and graph classification on four target domains.

Table 6: Analysis of one-shot node classification on homophilic and heterophilic graphs.

Target domain	Source domains	Accuracy (%)		
		GRAPHPROMPT	GCOPE	SAMGPT
Squi.	Cham., Corn., Cora	18.98±4.89	18.98±4.75	**20.43**±4.75
Corn.	Squi., Cham., Cora	29.67±8.36	27.19±8.51	**32.57**±8.68
Cham.	Squi., Corn., Cora	23.28±4.63	23.24±4.50	**23.89**±4.91
Facebook	Squi., Cora, Photo	32.22±6.91	35.81±7.89	**41.10**±9.38

Squi., Cham., Corn. are short for Squirrel, Chameleon, and Cornell, respectively.

the robustness of SAMGPT across domains with varying homophily patterns, we conduct one-shot node classification on homophilic (*Cora*, *Photo*, *Facebook*) and heterophilic (*Chameleon*, *Cornell* and *Squirrel*) graphs. Details about the heterophilic datasets are presented in Appendix F.

We report the results in Table 6 and observe that SAMGPT consistently surpasses GRAPHPROMPT and GCOPE, regardless of whether the source or target domains are homophilic or heterophilic. These results further validate the efficacy of SAMGPT, demonstrating its ability to leverage multi-domain knowledge across a wide variety of graph domains. Note that we focus on the node classification task here, as homophily is defined based on node attributes, which directly impacts node-level tasks.

6 Conclusions

In this paper, we proposed SAMGPT, a graph foundation model with structure alignment for text-free graphs, supporting both multi-domain graph pre-training and cross-domain adaptation. In the pre-training phase, SAMGPT utilizes a series of structure tokens to harmonize the structural distributions across multiple source domains and to extract multi-domain structural knowledge. For downstream cross-domain adaptation, SAMGPT employs dual prompts to tailor pre-trained holistic and domain-specific structural knowledge to the target domain. We conducted extensive experiments on seven benchmark datasets, demonstrating that SAMGPT significantly outperforms various state-of-the-art baseline methods.

Acknowledgments

This research / project is supported by the Ministry of Education, Singapore under its Academic Research Fund (AcRF) Tier 1 grant (22-SIS-SMU-054) and Tier 2 grant (Proposal ID: T2EP20122-0041). Any opinions, findings and conclusions or recommendations expressed in this material are those of the author(s) and do not reflect the views of the Ministry of Education, Singapore.

References

[1] Josh Achiam, Steven Adler, Sandhini Agarwal, Lama Ahmad, Ilge Akkaya, Florencia Leoni Aleman, Diogo Almeida, Janko Altenschmidt, Sam Altman, Shyamal Anadkat, et al. 2023. Gpt-4 technical report. *arXiv preprint arXiv:2303.08774* (2023).

[2] Vibhor Agarwal, Sagar Joglekar, Anthony P Young, and Nishanth Sastry. 2022. GraphNLI: A Graph-based Natural Language Inference Model for Polarity Prediction in Online Debates. In *WWW*. 2729–2737.

[3] Karsten M Borgwardt and Hans-Peter Kriegel. 2005. Shortest-path kernels on graphs. In *ICDM*. IEEE, 8–pp.

[4] Kaize Ding, Kai Shu, Xuan Shan, Jundong Li, and Huan Liu. 2021. Cross-domain graph anomaly detection. *IEEE TNNLS* 33, 6 (2021), 2406–2415.

[5] Junfeng Fang, Xinglin Li, Yongduo Sui, Yuan Gao, Guibin Zhang, Kun Wang, Xiang Wang, and Xiangnan He. 2024. EXGC: Bridging Efficiency and Explainability in Graph Condensation. In *WWW*. 721–732.

[6] Junfeng Fang, Wei Liu, Yuan Gao, Zemin Liu, An Zhang, Xiang Wang, and Xiangnan He. 2023. Evaluating Post-hoc Explanations for Graph Neural Networks via Robustness Analysis. In *Thirty-seventh Conference on Neural Information Processing Systems*.

[7] Taoran Fang, Yunchao Zhang, Yang Yang, Chunping Wang, and Lei Chen. 2023. Universal Prompt Tuning for Graph Neural Networks. In *NeurIPS*, Vol. 36.

[8] Christos Giatsidis, Fragkiskos Malliaros, Dimitrios Thilikos, and Michalis Vazirgiannis. 2014. CoreCluster: A degeneracy based graph clustering framework. In *AAAI*, Vol. 28.

[9] Kaveh Hassani. 2022. Cross-domain few-shot graph classification. In *AAAI*, Vol. 36. 6856–6864.

[10] Zhenyu Hou, Xiao Liu, Yukuo Cen, Yuxiao Dong, Hongxia Yang, Chunjie Wang, and Jie Tang. 2022. Graphmae: Self-supervised masked graph autoencoders. In *KDD*. 594–604.

[11] Ziniu Hu, Yuxiao Dong, Kuansan Wang, Kai-Wei Chang, and Yizhou Sun. 2020. Gpt-gnn: Generative pre-training of graph neural networks. *SIGKDD* (2020), 1857–1867.

[12] Xinke Jiang, Zidi Qin, Jiarong Xu, and Xiang Ao. 2023. Incomplete graph learning via attribute-structure decoupled variational auto-encoder. In *WSDM*. 304–312.

[13] Xinke Jiang, Rihong Qiu, Yongxin Xu, Wentao Zhang, Yichen Zhu, Ruizhe Zhang, Yuchen Fang, Xu Chu, Junfeng Zhao, and Yasha Wang. 2024. RAGraph: A General Retrieval-Augmented Graph Learning Framework. *NeurIPS* (2024).

[14] Thomas N Kipf and Max Welling. 2016. Variational graph auto-encoders. *arXiv preprint arXiv:1611.07308* (2016).

[15] Thomas N Kipf and Max Welling. 2017. Semi-supervised classification with graph convolutional networks. In *ICLR*.

[16] Jintang Li, Ruofan Wu, Wangbin Sun, Liang Chen, Sheng Tian, Liang Zhu, Changhua Meng, Zibin Zheng, and Weiqiang Wang. 2023. What's Behind the Mask: Understanding Masked Graph Modeling for Graph Autoencoders. In *KDD*. 1268–1279.

[17] Rongfan Li, Xinke Jiang, Ting Zhong, Goce Trajcevski, Jin Wu, and Fan Zhou. 2022. Mining spatio-temporal relations via self-paced graph contrastive learning. In *SIGKDD*. 936–944.

[18] Hao Liu, Jiarui Feng, Lecheng Kong, Ningyue Liang, Dacheng Tao, Yixin Chen, and Muhan Zhang. 2024. One for All: Towards Training One Graph Model for All Classification Tasks. In *ICLR*.

[19] Jiawei Liu, Cheng Yang, Zhiyuan Lu, Junze Chen, Yibo Li, Mengmei Zhang, Ting Bai, Yuan Fang, Lichao Sun, Philip S Yu, et al. 2023. Towards graph foundation models: A survey and beyond. *arXiv preprint arXiv:2310.11829* (2023).

[20] Zemin Liu, Yuan Fang, Chenghao Liu, and Steven CH Hoi. 2021. Relative and absolute location embedding for few-shot node classification on graph. In *AAAI*, Vol. 35. 4267–4275.

[21] Zemin Liu, Xingtong Yu, Yuan Fang, and Xinming Zhang. 2023. GraphPrompt: Unifying pre-training and downstream tasks for graph neural networks. In *WWW*. 417–428.

[22] Yuanfu Lu, Xunqiang Jiang, Yuan Fang, and Chuan Shi. 2021. Learning to pre-train graph neural networks. In *AAAI*, Vol. 35. 4276–4284.

[23] Chenglong Ma, Yongli Ren, Pablo Castells, and Mark Sanderson. 2024. Temporal Conformity-aware Hawkes Graph Network for Recommendations. In *WWW*. 3185–3194.

[24] Yao Ma, Xiaorui Liu, Neil Shah, and Jiliang Tang. 2022. Is homophily a necessity for graph neural networks?. In *ICLR*.

[25] Julian McAuley, Christopher Targett, Qinfeng Shi, and Anton Van Den Hengel. 2015. Image-based recommendations on styles and substitutes. In *SIGIR*. 43–52.

[26] Andrew Kachites McCallum, Kamal Nigam, Jason Rennie, and Kristie Seymore. 2000. Automating the construction of internet portals with machine learning. *Information Retrieval* 3 (2000), 127–163.

[27] Kentaro Miyake, Hiroyoshi Ito, Christos Faloutsos, Hirotomo Matsumoto, and Atsuyuki Morishima. 2024. NETEVOLVE: Social Network Forecasting using Multi-Agent Reinforcement Learning with Interpretable Features. In *WWW*. 2542–2551.

[28] Xuelian Ni, Fei Xiong, Yu Zheng, and Liang Wang. 2024. Graph Contrastive Learning with Kernel Dependence Maximization for Social Recommendation. In *WWW*. 481–492.

[29] Hongbin Pei, Bingzhe Wei, Kevin Chen-Chuan Chang, Yu Lei, and Bo Yang. 2020. Geom-GCN: Geometric graph convolutional networks. In *ICLR*.

[30] Jiezhong Qiu, Qibin Chen, Yuxiao Dong, Jing Zhang, Hongxia Yang, Ming Ding, Kuansan Wang, and Jie Tang. 2020. Gcc: Graph contrastive coding for graph neural network pre-training. In *SIGKDD*. 1150–1160.

[31] Faisal Rahutomo, Teruaki Kitasuka, Masayoshi Aritsugi, et al. 2012. Semantic cosine similarity. In *ICAST*, Vol. 4. 1.

[32] Ladislav Rampášek, Michael Galkin, Vijay Prakash Dwivedi, Anh Tuan Luu, Guy Wolf, and Dominique Beaini. 2022. Recipe for a general, powerful, scalable graph transformer. *NeurIPS* 35 (2022), 14501–14515.

[33] Benedek Rozemberczki, Carl Allen, and Rik Sarkar. 2021. Multi-scale attributed node embedding. *Journal of Complex Networks* 9, 2 (2021), cnab014.

[34] Benedek Rozemberczki and Rik Sarkar. 2020. Characteristic functions on graphs: Birds of a feather, from statistical descriptors to parametric models. In *CIKM*. 1325–1334.

[35] Prithviraj Sen, Galileo Namata, Mustafa Bilgic, Lise Getoor, Brian Galligher, and Tina Eliassi-Rad. 2008. Collective classification in network data. *AI magazine* 29, 3 (2008), 93–93.

[36] Oleksandr Shchur, Maximilian Mumme, Aleksandar Bojchevski, and Stephan Günnemann. 2018. Pitfalls of graph neural network evaluation. *arXiv preprint arXiv:1811.05868* (2018).

[37] Gilbert W Stewart. 1993. On the early history of the singular value decomposition. *SIAM review* 35, 4 (1993), 551–566.

[38] Fan-Yun Sun, Jordan Hoffman, Vikas Verma, and Jian Tang. 2019. InfoGraph: Unsupervised and Semi-supervised Graph-Level Representation Learning via Mutual Information Maximization. In *ICLR*.

[39] Mingchen Sun, Kaixiong Zhou, Xin He, Ying Wang, and Xin Wang. 2022. Gppt: Graph pre-training and prompt tuning to generalize graph neural networks. In *SIGKDD*. 1717–1727.

[40] Xiangguo Sun, Hong Cheng, Jia Li, Bo Liu, and Jihong Guan. 2023. All in One: Multi-Task Prompting for Graph Neural Networks. *SIGKDD* (2023), 2120–2131.

[41] Jiabin Tang, Yuhao Yang, Wei Wei, Lei Shi, Long Xia, Dawei Yin, and Chao Huang. 2024. HiGPT: Heterogeneous Graph Language Model. In *SIGKDD*. 2842–2853.

[42] Hugo Touvron, Thibaut Lavril, Gautier Izacard, Xavier Martinet, Marie-Anne Lachaux, Timothée Lacroix, Baptiste Rozière, Naman Goyal, Eric Hambro, Faisal Azhar, et al. 2023. Llama: Open and efficient foundation language models. *arXiv preprint arXiv:2302.13971* (2023).

[43] Petar Veličković, Guillem Cucurull, Arantxa Casanova, Adriana Romero, Pietro Lio, and Yoshua Bengio. 2018. Graph attention networks. In *ICLR*.

[44] Petar Veličković, William Fedus, William L Hamilton, Pietro Liò, Yoshua Bengio, and R Devon Hjelm. 2018. Deep Graph Infomax. In *ICLR*.

[45] Chen Wang, Yueqing Liang, Zhiwei Liu, Tao Zhang, and S Yu Philip. 2021. Pre-training graph neural network for cross domain recommendation. In *CogMI*. 140–145.

[46] Ning Wang, Minnan Luo, Kaize Ding, Lingling Zhang, Jundong Li, and Qinghua Zheng. 2020. Graph Few-shot Learning with Attribute Matching. In *CIKM*. 1545–1554.

[47] Qizhou Wang, Guansong Pang, Mahsa Salehi, Wray Buntine, and Christopher Leckie. 2023. Cross-domain graph anomaly detection via anomaly-aware contrastive alignment. In *AAAI*, Vol. 37. 4676–4684.

[48] Zeyuan Wang, Qiang Zhang, HU Shuang-Wei, Haoran Yu, Xurui Jin, Zhichen Gong, and Huajun Chen. 2022. Multi-level Protein Structure Pre-training via Prompt Learning. In *ICLR*.

[49] Zhihao Wen and Yuan Fang. 2023. Augmenting Low-Resource Text Classification with Graph-Grounded Pre-training and Prompting. In *SIGIR*. 506–516.

[50] Zhihao Wen and Yuan Fang. 2024. Prompt tuning on graph-augmented low-resource text classification. *IEEE TKDE* (2024).

[51] Zonghan Wu, Shirui Pan, Fengwen Chen, Guodong Long, Chengqi Zhang, and S Yu Philip. 2020. A comprehensive survey on graph neural networks. *IEEE TNNLS* 32, 1 (2020), 4–24.

[52] Jun Xia, Lirong Wu, Jintao Chen, Bozhen Hu, and Stan Z Li. 2022. Simgrace: A simple framework for graph contrastive learning without data augmentation. In *WWW*. 1070–1079.

[53] Lianghao Xia, Ben Kao, and Chao Huang. 2024. Opengraph: Towards open graph foundation models. *arXiv preprint arXiv:2403.01121* (2024).

[54] Minghao Xu, Hang Wang, Bingbing Ni, Hongyu Guo, and Jian Tang. 2021. Self-supervised graph-level representation learning with local and global structure. In *ICML*. 11548–11558.

[55] Baoyao Yang and Pong C Yuen. 2019. Cross-domain visual representations via unsupervised graph alignment. In *AAAI*, Vol. 33. 5613–5620.

[56] Chengxuan Ying, Tianle Cai, Shengjie Luo, Shuxin Zheng, Guolin Ke, Di He, Yanming Shen, and Tie-Yan Liu. 2021. Do transformers really perform badly for graph representation? *NeurIPS* 34 (2021), 28877–28888.

[57] Yuning You, Tianlong Chen, Yongduo Sui, Ting Chen, Zhangyang Wang, and Yang Shen. 2020. Graph contrastive learning with augmentations. *NeurIPS* 33

(2020), 5812–5823.

[58] Xingtong Yu, Yuan Fang, Zemin Liu, Yuxia Wu, Zhihao Wen, Jianyuan Bo, Xinming Zhang, and Steven CH Hoi. 2024. Few-Shot Learning on Graphs: from Meta-learning to Pre-training and Prompting. *arXiv preprint arXiv:2402.01440* (2024).

[59] Xingtong Yu, Zhenghao Liu, Yuan Fang, Zemin Liu, Sihong Chen, and Xinming Zhang. 2024. Generalized Graph Prompt: Toward a Unification of Pre-Training and Downstream Tasks on Graphs. *IEEE TKDE* (2024).

[60] Xingtong Yu, Zemin Liu, Yuan Fang, and Xinming Zhang. 2023. Learning to count isomorphisms with graph neural networks. *AAAI* 37, 4 (2023), 4845–4853.

[61] Xingtong Yu, Zemin Liu, Yuan Fang, and Xinming Zhang. 2024. HGPROMPT: Bridging Homogeneous and Heterogeneous Graphs for Few-shot Prompt Learning. In *AAAI*. 16578–16586.

[62] Xingtong Yu, Zhenghao Liu, Yuan Fang, and Xinming Zhang. 2025. Node-Time Conditional Prompt Learning in Dynamic Graphs. In *ICLR*.

[63] Xingtong Yu, Jie Zhang, Yuan Fang, and Renhe Jiang. 2025. Non-Homophilic Graph Pre-Training and Prompt Learning. In *SIGKDD*.

[64] Xingtong Yu, Chang Zhou, Yuan Fang, and Xinming Zhang. 2024. MultiGPrompt for Multi-Task Pre-Training and Prompting on Graphs. In *WWW*. 515–526.

[65] Xingtong Yu, Chang Zhou, Yuan Fang, and Xinming Zhang. 2024. Text-Free Multi-domain Graph Pre-training: Toward Graph Foundation Models. *arXiv preprint arXiv:2405.13934* (2024).

[66] Seongjun Yun, Minbyul Jeong, Raehyun Kim, Jaewoo Kang, and Hyunwoo J Kim. 2019. Graph transformer networks. *NeurIPS* 32 (2019).

[67] Delvin Ce Zhang, Menglin Yang, Rex Ying, and Hady W Lauw. 2024. Text-attributed graph representation learning: Methods, applications, and challenges. In *WWW*. 1298–1301.

[68] Lvmin Zhang, Anyi Rao, and Maneesh Agrawala. 2023. Adding conditional control to text-to-image diffusion models. In *ICCV*. 3836–3847.

[69] Haihong Zhao, Aochuan Chen, Xiangguo Sun, Hong Cheng, and Jia Li. 2024. All in one and one for all: A simple yet effective method towards cross-domain graph pretraining. In *SIGKDD*. 4443–4454.

[70] Jianan Zhao, Meng Qu, Chaozhuo Li, Hao Yan, Qian Liu, Rui Li, Xing Xie, and Jian Tang. 2023. Learning on Large-scale Text-attributed Graphs via Variational Inference. In *ICLR*.

[71] Jiong Zhu, Yujun Yan, Lingxiao Zhao, Mark Heimann, Leman Akoglu, and Danai Koutra. 2020. Beyond homophily in graph neural networks: Current limitations and effective designs. *NeurIPS* (2020), 7793–7804.

[72] Yun Zhu, Yaoke Wang, Haizhou Shi, Zhenshuo Zhang, Dian Jiao, and Siliang Tang. 2024. GraphControl: Adding Conditional Control to Universal Graph Pre-trained Models for Graph Domain Transfer Learning. In *WWW*. 539–550.

Appendices

A Algorithm

Our algorithm consists of two stages, multi-domain graph pre-training and downstream adaptation.

In the multi-domain pre-training phase, we first apply the dimension alignment function, DAL, to align feature dimensions from different source domains by Eq. (3). Then, we use a feature alignment method to unify feature semantic spaces by Eq. (4). For structure alignment, we inject source domain-specific structure tokens into each layer of the graph encoder by Eq. (6). Finally, we fuse the feature aligned embedding and structure aligned embedding by Eq. (7), and optimize the pre-training loss by Eq. (8).

We further present the key steps for cross-domain adaptation in Algorithm 1. In lines 3–4, we align target domain feature dimensions with source domains. In lines 6–7, we integrate the feature adaptation method to generate feature-level adapted embeddings. In lines 8–21, we employ dual prompts to adapt structural prior knowledge to the target domain. Specifically, we first inject holistic prompts to modify the structure-based aggregation in each layer of the graph encoder for holistic knowledge adaptation (lines 9–12). Then, we generate specific prompts by fusing the pre-trained structure tokens (lines 13–15), and utilize specific prompts for domain-specific knowledge adaptation (lines 17–19). We obtain structure-level adapted embeddings by fusing holistic and domain-specific embeddings (lines 20–21), and generate final embeddings by aggregating feature- and structure-level adapted embeddings (lines 22–23). Finally, we update the embeddings for the prototypical instances based on the labeled samples in the task and optimize holistic prompts, Λ and Γ (lines 24-28).

B Complexity Analysis

For a downstream graph $G_T = (V_T, E_T, \mathbf{X}_T)$ from the target domain D_T, the computational process of structure adaptation involves injecting holistic prompts and specific prompts into the pre-trained GNN to modify the encoding of nodes.

In a standard GNN, each node aggregates messages from its neighbors in each layer. Assuming that the aggregation involves at most n neighbors, the complexity of calculating node embeddings over L layers is $O(n^L \cdot |V_T|)$. One one hand, holistic prompts are directly injected into each layer of the GNN, increasing the complexity by $O(L \cdot |V_T|)$. On the other hand, specific prompts are first generated by the pre-trained structure tokens from K source domains, with an additional complexity of $O(L \cdot K)$. Then, specific prompts modify the structure-base aggregation with a complexity of $O(L \cdot |V_T|)$. Since holistic prompts and specific prompts modifies

Algorithm 1 Cross-domain Adaptation for SAMGPT

```
Input: Pre-trained graph encoder GE with parameters $\Theta_{\text{pre}}$, pre-trained
    structure tokens $\mathcal{T}_{\text{pre}}$, target domain dimension alignment function
    $\texttt{DA}_T(\cdot)$, and feature adaptation function $\texttt{FAD}(\cdot)$
Output: Optimized holistic prompts $\mathcal{P}_{\text{hol}}$, coefficients $\Lambda$, and feature adap-
    tation parameters $\Gamma$
1:  while not converged do
2:      for each graph $G_T = (V_T, E_T, \mathbf{X}_T)$ in target domain $D_T$ do
3:          /* Target domain feature dimensions alignment by Eq. (3) */
4:          $\tilde{\mathbf{X}} \leftarrow \texttt{DAL}_T(\mathbf{X})$
5:          $\mathcal{P}_{\text{hol}}, \Lambda, \Gamma \leftarrow$ initialization
6:          /* Feature adaptation by Eq. (5) */
7:          $\mathbf{H}^{\texttt{FAD}} \leftarrow \texttt{GE}(\texttt{FAD}(\mathcal{G}, \tilde{\mathbf{X}}; \Gamma); \Theta_{\text{pre}})$
8:          /* Structure alignment by dual prompts */
9:          /* Modification to GE via holistic prompts by Eq. (9) */
10:         for each layer in GE do
11:             $\mathbf{h}_v^l \leftarrow \texttt{Aggr}(\mathbf{h}_v^{l-1}, \{\mathbf{p}_{\text{hol}}^l \odot \mathbf{h}_u^{l-1} : u \in \mathcal{N}_v\}; \theta_{\text{pre}}^l), \ \forall v \in G_T$
12:         $\mathbf{H}^{\text{hol}} \leftarrow \texttt{STACK}(\{\mathbf{h}_v : \ \forall v \in G_T\})$
13:         /* Generation of specific prompts by Eq. (10) */
14:         for $\mathbf{p}_{\text{spe}}^l$ in $\mathcal{P}_{\text{spe}}$ do
15:             $\mathbf{p}_{\text{spe}}^l \leftarrow \sum_{i=1}^{K} \lambda_i^l \mathbf{t}_{S_i}^l$
16:         /* Modification to GE via specific prompts*/
17:         for Each layer in GE do
18:             $\tilde{\mathbf{h}}_v^l \leftarrow \texttt{Aggr}(\tilde{\mathbf{h}}_v^{l-1}, \{\mathbf{p}_{\text{spe}}^l \odot \tilde{\mathbf{h}}_u^{l-1} : u \in \mathcal{N}_v\}; \theta_{\text{pre}}^l), \ \forall v \in G_T$
19:         $\mathbf{H}^{\text{spe}} \leftarrow \texttt{STACK}(\{\tilde{\mathbf{h}}_v : \ \forall v \in G_T\})$
20:         /* Fusion of dual-prompt tuned embeddings by Eq. (11) */
21:         $\mathbf{H}^{\text{SAD}} \leftarrow \mathbf{H}^{\text{hol}} + \beta \mathbf{H}^{\text{spe}}$
22:         /* Fusion of adapted embeddings by Eq. (12) */
23:         $\mathbf{H}^{\texttt{AD}} \leftarrow \mathbf{H}^{\texttt{FAD}} + \alpha \mathbf{H}^{\text{SAD}}$
24:         /* Update prototypical nodes */
25:         for each class $y$ do
26:             $\mathbf{h}_y \leftarrow \textsc{Mean}(\{\mathbf{h}_x\text{: instance } x \text{ belongs to class } y\})$
27:         /* Optimizing $\mathcal{P}_{\text{hol}}$, $\Lambda$, and $\Gamma$ */
28:         Calculate $\mathcal{L}_{\text{down}}(\Omega; \mathcal{P}_{\text{hol}}, \Lambda, \Gamma)$ by Eq. (13)
29: return $\mathcal{P}_{\text{hol}}$, $\Lambda$, and $\Gamma$
```

the node encoding phase separately, the overall complexity would increase by $(L \cdot |V_T| + L \cdot K)$.

Thus, the encoding time by the pre-trained GNN still dominates the overall complexity, as $O(n^L \cdot |V_T|)$ typically exceeds $O(L \cdot |V_T| + L \cdot K)$ given that $n^L > L$ and $|V_T| > K$ in general. In other words, our structural adaptation adds a marginal overhead to the pre-trained graph encoder.

C Further Descriptions of Datasets

In this section, we provide more comprehensive descriptions of the benchmark datasets used in our experiments, as summarized in Table 1, in the following.

- *Cora* [26] consists of 2,708 publications in the computing field, each categorized into one of seven classes. The citation network comprises 5,429 edges. Each publication is represented by a binary word vector indicating the presence or absence of words from a dictionary containing 1,433 unique words.
- *Citeseer*[35] contains 3,312 computer science publications, each belonging to one of six categories, distinct from those in *Cora*. The citation network consists of 4,732 edges. Each publication is represented by a binary word vector, reflecting the presence or absence of words from a dictionary of 3,703 unique words.
- *PubMed* [35] consists of 19,717 biomedical publications related to diabetes, each classified into one of three categories. The citation network includes 44,338 edges. Each publication is represented by a TF/IDF-weighted word vector, indicating the presence of 500 unique words from the dictionary.
- *Photo* [36] contains 7,487 products related to photography, each assigned to one of eight categories. The co-purchase network comprises 119,043 edges, representing products frequently bought together. Each product is described by a feature vector derived from its metadata and reviews, and is labeled according to its category.
- *Computers* [36] includes 13,752 computer-related products, divided into ten categories. The co-purchase network consists of 245,861 edges, representing products that are frequently bought together. Each product is characterized by a feature vector generated from its metadata and reviews and is labeled according to its respective category.
- *Facebook* [33] represents a page-to-page Web graph of verified Facebook pages. The nodes correspond to official Facebook pages, and the edges indicate mutual "likes" between these pages. Node features are derived from the descriptions provided by the page owners that outline the purpose of their pages.
- *LastFM* [34] represents a social network of LastFM users, collected via the public API in March 2020. The nodes correspond to LastFM users from various Asian countries, and the edges represent mutual follower relationships. The node features are extracted based on the artists that users have liked. The associated task for this graph is multinomial node classification, where the objective is to predict each user's location, derived from the country field in their profile.

D Further Descriptions of Baselines

In this section, we provide additional details about the baselines used in our experiments.

(1) End-to-end GNNs:

- **GCN** [15]: GCN employs a mean-pooling approach for neighborhood aggregation, enabling the integration of information from adjacent nodes.
- **GAT** [43]: GAT relies on neighborhood aggregation for node representation learning, but distinguishes itself by assigning varying attention weights to neighbors, thus adjusting their influence on the aggregation process.

(2) Graph pre-training models:

- **DGI** [43]: DGI is a self-supervised pre-training approach. It is based maximizing mutual information (MI), with the goal of strengthening the MI between local node representations and their global context.
- **InfoGraph** [38]: Building on DGI, InfoGraph focuses on graph-level tasks, aiming to align node and graph embeddings by maximizing the similarity between them.
- **GraphCL** [57]: GraphCL applies various graph augmentations for self-supervised learning, leveraging structural patterns within graphs. Its main objective is to improve the similarity across different augmentations during pre-training.
- **GPPT** [39]: GPPT pre-trains a GNN model via link prediction task. Its downstream prompt module is specifically designed for node classification, unifying it with the pre-training link prediction task.
- **GPF** [7]: GPF serves as a universal prompt-based tuning approach for pre-trained graph models. It adapts the input graph's feature space to simulate the behavior of various prompting functions.
- **GraphPrompt** [21]: GraphPrompt utilizes subgraph similarity calculations as a unified framework to bridge the gap between pre-training and downstream tasks, supporting both node and graph classification. During downstream adaptation, a learnable prompt is tuned to incorporate task-specific knowledge.

(3) Graph cross-domain models:

- Hassani [9]: Hassani proposes an attention-based graph encoder that leverages both contextual and topological views to capture task-specific information for quick adaptation, as well as task-independent knowledge for efficient transfer across domains.

(4) Multi-domain graph pre-training models:

- **GCOPE** [69]: GCOPE propose a multi-domain pre-training strategy that integrates graph datasets from various domains using domain-specific interconnecting virtual nodes, which link nodes within the same domain. The main objective is to enhance downstream performance by harnessing knowledge from multiple source domains.

E Implementation Details

We outline key settings for the baselines and SAMGPT.

Baseline settings. We utilized the official codes for all open-source baselines. Each model was tuned based on the settings recommended in their respective work to achieve optimal performance.

For the baseline GCN [15], we employ a 3-layer architecture, and set the hidden dimensions to 256. For GAT [43], we employ a 2-layer architecture and set the hidden dimension to 64. Additionally, we apply 8 attention heads in the first GAT layer.

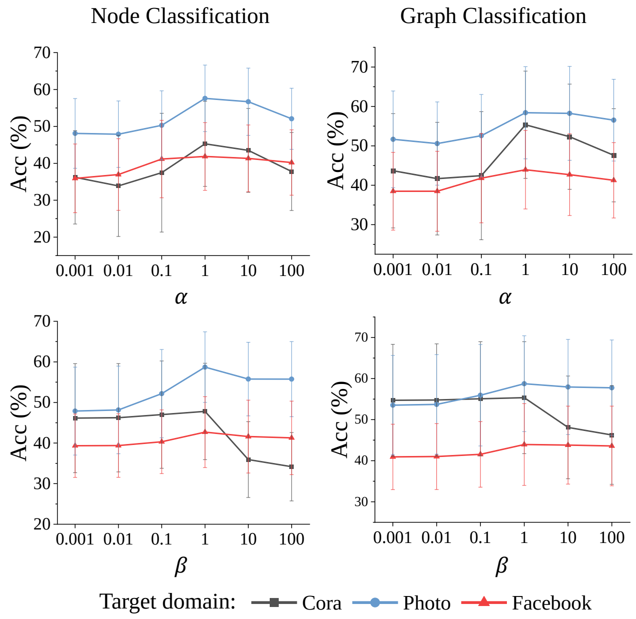

Figure 4: Sensitivity study of α and β.

For DGI [43], we utilize a 1-layer GCN as the backbone and set the hidden dimensions to 256. Additionally, we employ prelu as the activation function. For InfoGraph [38], a 3-layer GCN is used as the backbone, with its hidden dimensions set to 256. For GraphCL [57], a 1-layer GCN is also employed as its backbone, with the hidden dimensions set to 256. Specifically, we select edge dropping as the augmentations, with a default augmentation ratio of 0.2. For GPPT [39], we utilize a 2-layer GraphSAGE as its backbone, setting the hidden dimensions to 256. We employ a mean aggregator for the aggregation in the backbone. For GraphPrompt [21], a 3-layer GCN is used as the backbone for all datasets, with the hidden dimensions set to 256. For GPF [7], we employ a 5-layer GCN as the backbone for all datasets, following the recommended settings. The hidden dimensions are set to 256.

For Hassani [9], a 3-layer GCN is used as the backbone for all datasets, with the hidden dimensions set to 256.

For GCOPE [69], we employ a 2-layer GCN as the backbone and set the hidden dimensions to 100. Downstream adaptation is achieved through fine-tuning, as it is reported to yield the best performance in their literature.

For all baselines except GCOPE, we set the unified feature dimensions to 50, matching our SAMGPT. For GCOPE, we adhere to the recommended settings and set it to 100.

SAMGPT settings. For our proposed SAMGPT, we utilize a 3-layer GCN as the backbone for all datasets, with the hidden dimensions set to 256. We set the unified feature dimensions to 50.

F Details about Heterophilic Datasets

To evaluate the robustness of SAMGPT across graphs with varying homophily ratios, we conducted experiments on both homophilic and heterophilic datasets in Sect. 5.4. Details of the heterophilic datasets are introduced as follows. (1) *Chameleon* [33] is a Wikipedia-based network containing 2,277 pages, categorized into five groups based on their average monthly traffic. This dataset forms a network with 36,101 edges, and the node features are derived from key nouns extracted from the Wikipedia content. (2) *Cornell* [29] is another webpage network consisting of 183 nodes, where each node represents a webpage, and 295 edges denoting hyperlinks between them. The node features are derived from a bag-of-words representation of the webpages. These pages are manually classified into five categories: student, project, course, staff, and faculty. (3) *Squirrel* [33] consists of 5,201 Wikipedia pages discussing specific topics. The pages are divided into five categories based on their average monthly traffic. This dataset forms a page-to-page network with 217,073 edges, and the node features are derived from various informative nouns present in the Wikipedia content.

G Hyperparameter Sensitivity

We investigate the impact of hyperparameters, α and β, in SAMGPT. α governs the fusion of feature and structure alignment, as well as their adaptation, in Eqs. (7) and (12), whereas β controls the aggregation of holistic and domain-specific adaptation in Eq. (11). We vary α and β and present 1-shot node and graph classification results on three target domain, *Cora*, *Photo* and *Facebook*, in Fig. 4, with error bars denoting the standard deviation.

We observe that increasing α from lower values initially enhances performance as structure alignment and adaptation are emphasized. However, after reaching a peak ($\alpha = 1$), accuracy begins to decline as α grows further, implying that both feature and structure alignment are essential. Moreover, β exhibit a trend similar to that of α, demonstrating that incorporating both holistic and domain-specific knowledge is vital for cross-domain adaptation. Based on the above observations, we set $\alpha = 1$ in our experiments, indicating a balance between the feature and structure counterparts, and $\beta = 1$, indicating a balance between holistic and specific prompts, both of which show robust empirical performance.

H Data Ethics Statement

To evaluate the efficacy of SAMGPT, we conducted experiments with only publicly available datasets, including Cora[3], Citeseer[4], Pubmed[5], Photo[6], Computers[7], Facebook[8], LastFM[9], Chameleon[10], Cornell[11], and Squirrel[12] in accordance to their usage terms and conditions, if any. We also confirm that no personally identifiable information was utilized, and this research did not involve any human or animal subjects.

[3] https://github.com/shchur/gnn-benchmark/raw/master/data/npz/cora.npz
[4] https://github.com/shchur/gnn-benchmark/raw/master/data/npz/citeseer.npz
[5] https://github.com/shchur/gnn-benchmark/raw/master/data/npz/pubmed.npz
[6] https://github.com/shchur/gnn-benchmark/raw/master/data/npz/amazon_electronics_photo.npz
[7] https://github.com/shchur/gnn-benchmark/raw/master/data/npz/amazon_electronics_computers.npz
[8] https://graphmining.ai/datasets/ptg/facebook.npz
[9] https://graphmining.ai/datasets/ptg/lastfm_asia.npz
[10] https://github.com/SitaoLuan/ACM-GNN/tree/main/new_data/chameleon
[11] https://github.com/bingzhewei/geom-gcn/tree/master/new_data/cornell
[12] https://github.com/SitaoLuan/ACM-GNN/tree/main/new_data/squirrel